Measurement of Characteristic Length of Nonlocal Continuum

By Zdeněk P. Bažant,[1] Fellow, ASCE, and Gilles Pijaudier-Cabot,[2] Associate Member, ASCE

Abstract: The characteristic length of a heterogeneous brittle material such as concrete represents a material property that governs the minimum possible width of a zone of strain-softening damage in nonlocal continuum formulations or the minimum possible spacing of cracks in discrete fracture models. This length is determined experimentally. The basic idea is to compare the response of two types of specimens, one in which the tensile softening damage remains distributed and one in which it localizes. The latter type of specimen is an edge-notched tensile fracture specimen, and the former type of specimen is of the same shape but without notches. Localization of softening damage is prevented by gluing to the specimen surface a layer of parallel thin-steel rods and using a cross section of a minimum possible thickness that can be cast with a given aggregate. The characteristic length l is the ratio of the fracture energy (i.e., the energy dissipated per unit area, dimension N/m) to the energy dissipated per unit volume (dimension N/m^2). Evaluation of these energies from the present tests of concrete yields $l \simeq 2.7$ times the maximum aggregate size.

Introduction

From a number of recent studies (e.g., Bažant 1986; Bažant and Pijaudier-Cabot 1987a, 1987b) it transpires that mathematical modeling of softening damage, such as cracking or void formation, necessitates a certain length parameter that is a property of the material and is called the characteristic length l. Although the characteristic length has been used in various nonlocal models for strain-softening, its value has so far been estimated only indirectly, probably with considerable uncertainty. No measurements of this essential parameter have yet been made. To present such measurements is the objective of this study [which is based on a report and a conference paper by Bažant and Pijaudier-Cabot (1987b, 1988)].

Depending on the type of material model, the characteristic length can have two interpretations:

1. If the softening damage is modeled by means of a strain-softening continuum, it is necessary to use some type of a localization limiter which prevents the damage zone from localizing to a zero volume. Thus, there must be a certain minimum thickness of the localization region that is related to the characteristic length of the continuum. This is in general described by a nonlocal continuum, in which certain strain variables are determined by averaging over the neighborhood of a point, the size of the neighborhood being determined by the characteristic length. Without the characteristic length, the strain-softening models for damage can correctly describe only the situations where the damage remains distributed, not the situations where the damage tends to localize.

2. The discrete crack models with a softening cohesive zone at the crack front, introduced for concrete by Hillerborg et al. (1976), can correctly describe localized cracking or damage, but may yield ambiguous results for situations where damage or cracking remains distributed (Bažant 1986). Such situations include, in statics, certain problems of cracking due to cooling or shrinkage, or problems where a compression zone lies closely ahead of the cracking front (as in bending), and problems of cracking in reinforced materials. In dynamics, localization of damage into a single crack may be prevented for a certain period of time by inertia effects. The same may occur in statics when the strain-rate sensitivity of the material is introduced. To describe such situations, the discrete crack models must contain a material length parameter that indicates the minimum possible spacing of the cracks. This parameter is equivalent to the aforementioned characteristic length l, and the discrete and continuum models give roughly the same results if the displacement used in the stress-displacement softening relation for the cohesive zone of a crack is made equal to $l\epsilon$, where ϵ = the strain used in the softening stress-strain relation of a nonlocal continuum.

To determine the characteristic length, the basic idea is to measure the response of two types of specimens that are as similar as possible but such that in one type of specimen the damage, such as cracking, remains nearly homogeneously distributed, while in the other type, it localizes to the minimum volume that is possible for the given material. We will describe the development of such specimens and testing results, and then proceed to analyze the test results to obtain the characteristic length of concrete.

Test Specimens and Measurement Method

The fact that a tensile specimen that is forced by an elastic restraint to deform homogeneously exhibits a gradual post-peak strain-softening and has a higher strength than an unrestrained tensile specimen was discovered by L'Hermite (1960). With his coworkers, he tested specimens made by casting concrete into a steel pipe with an internal thread. Bonded to concrete by the thread, the steel pipe was loaded in tension and transmitted the tensile force to the concrete. Since the pipe was elastic, the force it carried was easily determined by measuring the deformation of the pipe, and the remainder of the tensile force could be ascribed to the concrete. The steel pipe no doubt prevented the tensile cracking from localizing into a single major crack. Companion tests in which concrete was bonded to the pipe only near the grips revealed significant differences in the strength limit and the post-peak behavior.

L'Hermite's tests, however, had a drawback due to the fact that the steel envelope has a higher Poisson ratio than concrete. As a result, the concrete in the pipe must have been subjected in these tests to significant lateral compressive stresses producing a confinement effect. Therefore, these tests cannot be regarded as uniaxial; and the presence of triaxial stresses complicates interpretation of the measurements.

As a modification of L'Hermite's idea, one might think of achieving a homogeneous strain state in tension by testing tensile specimens reinforced

[1]Prof. of Civ. Engrg., Northwestern Univ., Evanston, IL 60208.
[2]Res. Assoc., Dept. of Civ. Engrg., Rensselaer Polytech. Inst., Troy, NY 12181; formerly, Grad. Res. Asst., Northwestern Univ., Evanston, IL.

Note. Discussion open until September 1, 1989. To extend the closing date one month, a written request must be filed with the ASCE Manager of Journals. The manuscript for this paper was submitted for review and possible publication on March 10, 1988. This paper is part of the *Journal of Engineering Mechanics*, Vol. 115, No. 4, April, 1989. ©ASCE, ISSN 0733-9399/89/0004-0755/$1.00 + $.15 per page. Paper No. 23365.

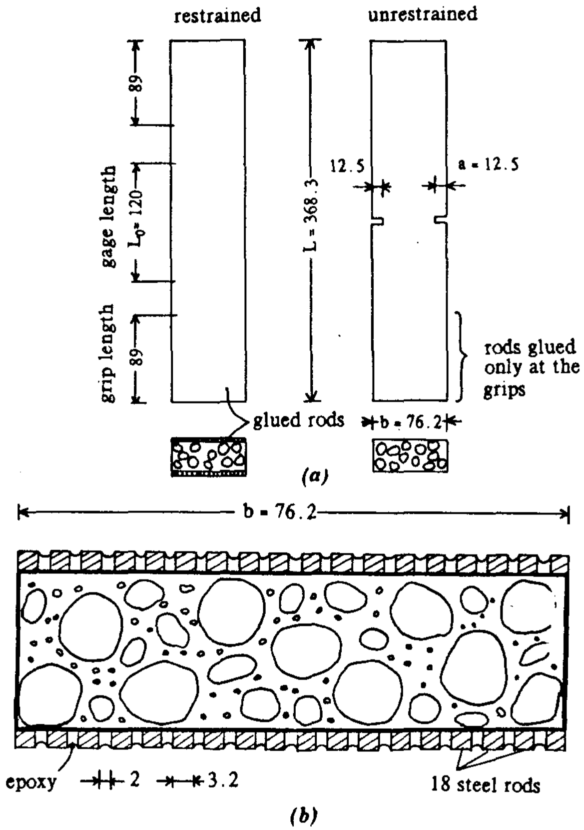

FIG. 1. (a) Notched and Unnotched Specimen Tested; (b) Arrangement of Steel Bars at Surface of Concrete (All Dimensions in mm)

by longitudinal steel bars instead of the pipe. However, due to the fact that the interface area between steel bars and concrete is relatively small and the bond is imperfect, a uniform strain state in reinforced tensile specimens is usually not achieved. A further source of nonuniformity may again be the difference of Poisson ratios between concrete and steel.

Alternatively, distributed cracking can be more easily achieved in specimens subjected to bending, due to the restraining effect of the compressed concrete layer in bent specimens. The nonuniformity of strain across the beam, however, complicates interpretation of the results. Moreover, the presence of a transverse strain gradient causes the tensile strength in bent specimens to be higher than in a uniform tensile strain field (this effect is actually explicable by the nonlocal character of the material).

To achieve perfect bond, one might cast concrete first and then glue to its surface metallic sheets. However, the mismatch in Poisson ratios would still produce lateral stresses.

In view of the foregoing considerations, the restrained and unrestrained specimens shown in Fig. 1 were selected. As is seen in Fig. 1(*b*), the longer

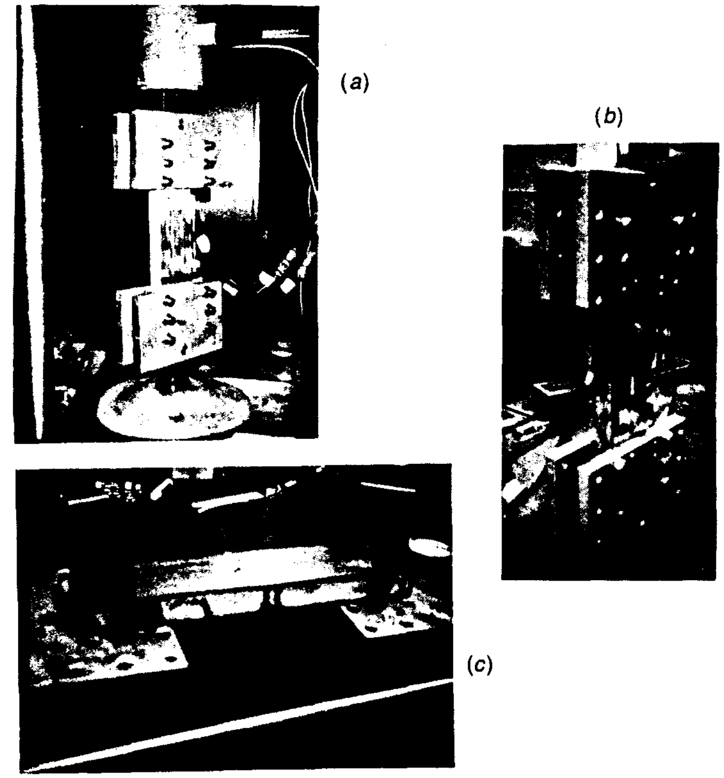

FIG. 2. Photographs of Specimen Tested

sides of the rectangular cross section are restrained by gluing to them with epoxy a system of regularly spaced, thin steel rods, which have relatively large gaps between them. These gaps, filled by epoxy, are quite deformable, because the elastic modulus of epoxy is much lower than that of concrete. Consequently, the set of thin steel rods cannot develop any significant transverse stresses and thus cannot interfere appreciably with the Poisson effect in concrete. Furthermore, by choosing the cross sections of the rods to be much smaller than the maximum aggregate size, the thin rods cannot affect the nonlocal properties of the material in the transverse direction. The rectangular cross section is elongated, so as to minimize the influence of the wall effect and the local stresses near the short sides of the cross section.

The thickness of the cross section was chosen to be only three times the maximum aggregate size. The reason for this was to ensure that the restraint due to the steel rods glued to the surface affects the entire thickness of the specimen. For much thicker specimens, the restraint of the interior would be incomplete, and the strains could localize in the middle of the thickness. Selection of a circular cross section of a diameter only three aggregate sizes would yield a specimen whose behavior would no doubt be statistically more scattered. By using an elongated rectangular cross section, the number of aggregate pieces in the cross section is considerably increased, causing the

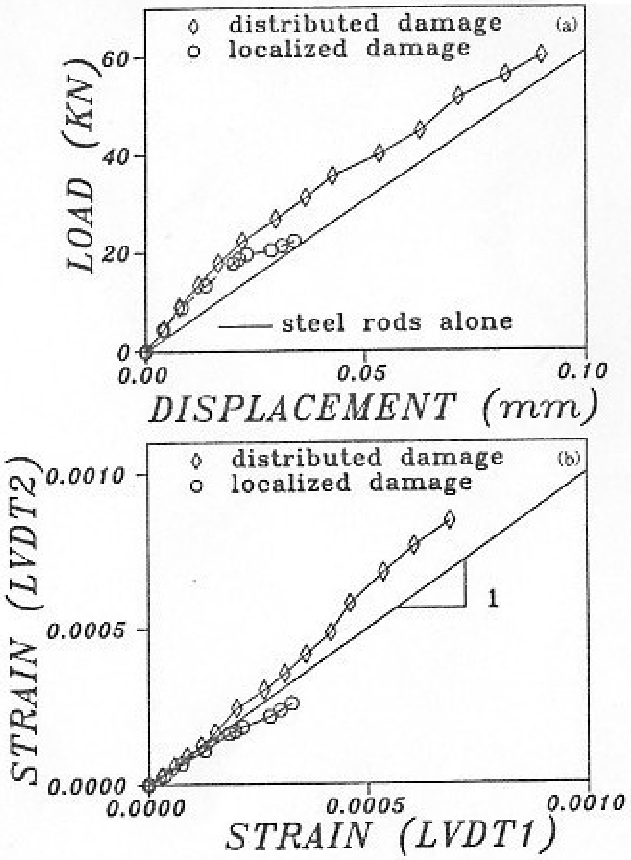

FIG. 3. (*a*) Load-Displacement Curves for Distributed and Localized Cracking Specimens; (*b*) Strains Measured on Each Side of Specimen

measured response, which roughly corresponds to the average property of the cross section, to be less scattered.

The dimensions of the specimen are all shown in Fig. 1 (in mm). The weight ratio of water-cement-sand-gravel in the mix was 1:2:2:0.6, and the maximum size of the aggregate was d_a = 9.53 mm. ASTM Type I cement was used. The specimens were removed from their plywood forms at 24 hours after casting and were then cured for 28 days in a room of relative humidity 95% and temperature 80° F.

At the ends of the specimen, metallic grips were glued by epoxy to the surface of the steel rods. In the companion unrestrained specimens, the surface steel rods were glued to the grips only within the area under the grips. To ensure that the tensile crack forms away from the grips and runs essentially normal to the axis, notches (of thickness 2.5 mm) were cut by a saw into the unrestrained specimens (Fig. 1).

The combined total cross section of the steel rods was selected so as to ensure that the tangential stiffness of both the restrained and the unrestrained specimen would always remain positive. Consequently, the stability of the

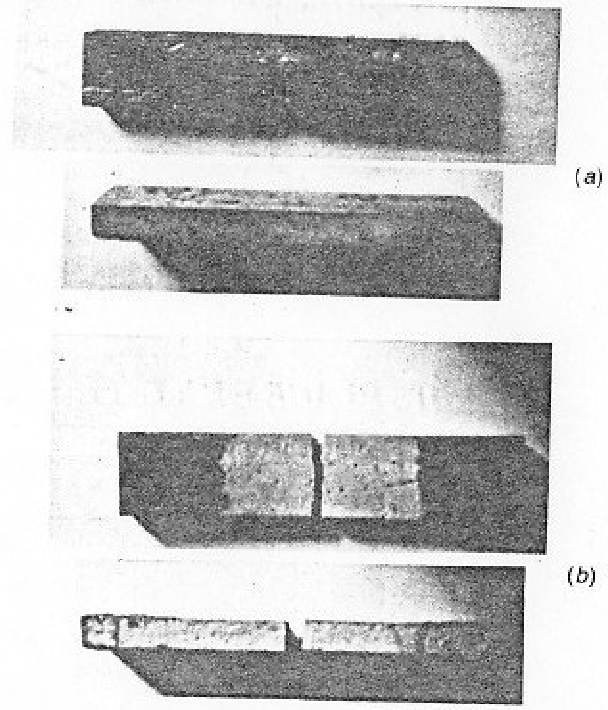

FIG. 4. Specimens after Failure: (*a*) Distributed Cracking; (*b*) Localized Cracking

specimen and strain localization could not depend on the stiffness of the testing machine.

The specimens were tested in tension in a closed-loop 100-kN MTS testing machine (Fig. 2). The loading was stroke controlled and was made at a constant displacement rate of 0.0038 mm/s, which produces the mean strain rate 2×10^{-5}/s. The relative displacements on a base length of 120 mm (Fig. 1) were measured by two symmetrically placed LVDT gages mounted on one face of the specimen and attached to the steel fibers (Fig. 2). Three specimens of each type were tested, but only two tests on unrestrained specimens could be exploited because of technical difficulties in setting up one of these experiments. Due to the small number of specimens, only the mean response is presented, and even the means might have considerable uncertainty. No conclusions on statistical variability can be drawn.

The plot of the average load versus displacement (mean of the measurements from the two LVDTs for each test) for the restrained and unrestrained specimens, which exhibit distributed and localized cracking, are shown in Fig. 3(*a*). The results confirm that the incremental stiffness has always been positive. It is seen that for the unrestrained specimens (unbonded rods), the load-displacement curve quickly approaches that for the steel rods alone. On the other hand, for the restrained specimens, the load displacement curve remains for a long time significantly higher than that for the steel rods alone.

No macrocracks were observed on the short exposed sides of the restrained specimens (see Fig. 4), but a series of tiny microcracks could be detected.

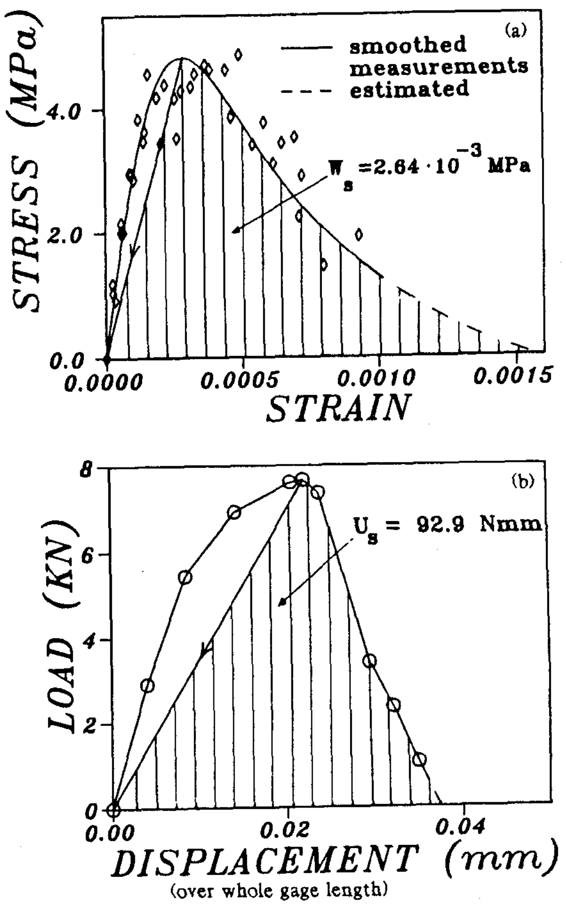

FIG. 5. (*a*) Stress-Strain Curve from Restrained Specimens; (*b*) Load-Displacement Curve from Unrestrained Specimens

It was also noticed that microcracking was somewhat more extensive farther away from the surface of the specimen. This may be explained by the restraint of the steel bars.

The results for the restrained specimens from Fig. 3 were converted to stress-strain curves for the restrained specimens with distributed damage [see Fig. 5(*a*)]. The final portion of the softening curve (shown dashed) had to be estimated by analogy with other test data. It may be noted that the relative scatter of the results in Fig. 5(*a*) is increased by the fact that the force in the steel is subtracted from the measured force values. This may explain why the measured response curve is not very smooth.

Fig. 3(*b*) shows the plot of the strains measured by the LVDT gages mounted on the left and right sides of the specimen. It may be noted that in the strain-softening range, these two strains become markedly different, so that the specimen deformation becomes asymmetric, i.e., the specimen undergoes

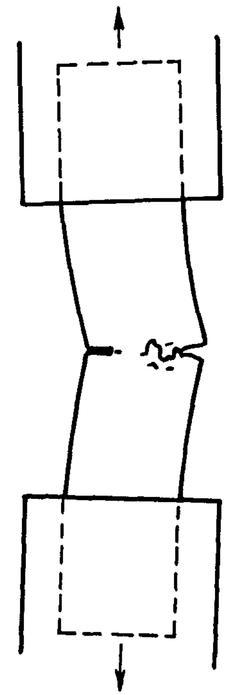

FIG. 6. Failure Mode of Unrestrained Specimens

bending, as shown in Fig. 6. This is not merely a consequence of random imperfections but is a manifestation of an instability that must occur in tensile fracture specimens of this type, as shown by Rots et al. (1987) and Hordijk et al. (1987). This implies that, in the unrestrained notched specimens, the cracking must propagate from one side of the cross section to the other, rather than happening simultaneously. The propagation of the cracking zone from one side of the specimen to the other helps to explain why the measurements indicate the maximum force carried by concrete in the unrestrained specimens to be considerably smaller than that in the restrained ones. However, even if the cracking zones propagated symmetrically, the fact that the failure cannot be simultaneous and that the specimen is notch-sensitive would require the maximum load to be less than that for the restrained specimen.

The test results for the unrestrained specimens with localized damage are plotted in Fig. 5(*b*) in terms of the average force *P*, carried by concrete versus the relative displacement *u* over the gage length. Interpretation in terms of the stress-strain curve is not attempted because the specimen state was inhomogeneous.

Calculation of Characteristic Length from Test Results

Taking the continuum viewpoint, we may consider the distributions of the macroscopic longitudinal normal strain along the gage length of the speci-

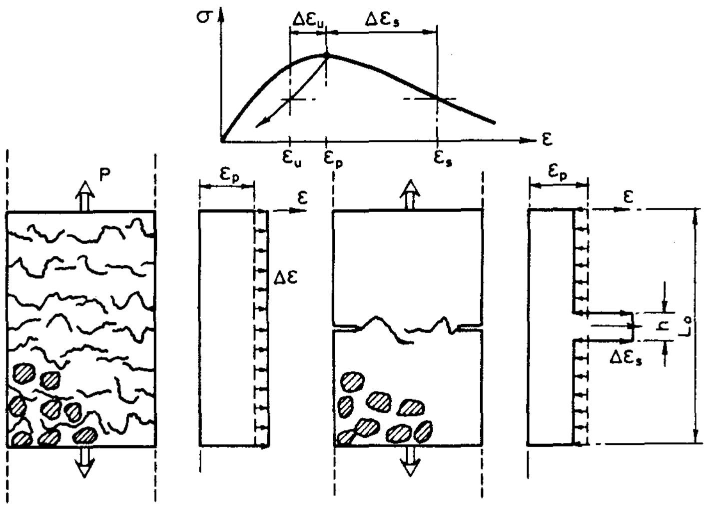

FIG. 7. Assumed Strain Distribution with and without Localization

men to be as shown in Fig. 7, i.e., uniform for the restrained specimen, and localized, with a piecewise constant distribution, for the unrestrained specimen. Further, we assume that this localization begins to develop right at the peak stress point, at which the strain is $\epsilon = \epsilon_p$, as shown in the stress-strain diagram in Fig. 7. Although the nonlocalized states are stable up to a certain point on the descending stress-strain curve (Bažant 1976, 1986), the localization must begin, in a stable manner, precisely at the peak stress. This can be proven thermodynamically, on the basis of maximization of internal entropy (Bažant 1987). The fact that localization begins precisely at the peak stress point has also been documented by some recent measurements of deformation distributions in tensile specimens (Raiss 1986).

The energy U_s that is dissipated due to fracturing in the unbonded specimen with localized strain is represented by the area under the curves of axial force P versus axial relative displacement u for loading and for unloading from the peak-stress point, as shown by the cross-hatched area in Fig. 5(*b*). This energy should not include the blank area between the loading stress-strain curve and the unloading stress-strain curve, as proven in Bažant (1982). The energy U_s dissipated by fracturing in the bonded specimen without strain localization must be determined in the same manner. This energy, representing the energy density, is shown by the cross-hatched area in Fig. 5(*a*).

We may now define the effective width h (Fig. 7) of the localized strain profile to be such that the stress-strain diagram for the localization zone (fracture process zone) would be the same as that for the bonded specimen with a homogeneous strain distribution. Thus, the balance of energy requires that $G_f = hW_s$, where $G_f = U_s/A_0$ = fracture energy of the material (dimension N/m); and A_0 = the area of the net (ligament) cross section of the notched specimen. From this, the effective width of the localization zone is obtained as

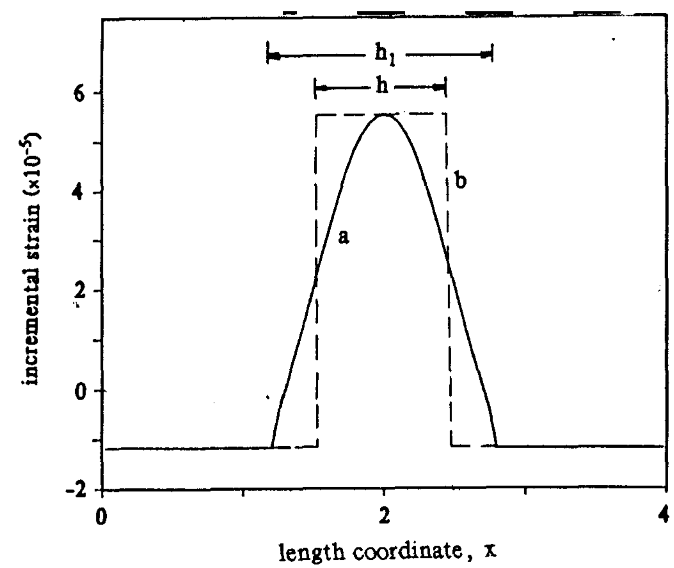

FIG. 8. Analytical Strain Profile at Localization Instability (after Bažant and Pijaudier-Cabot 1987)

$$h = \frac{G_f}{W_s} \quad (1)$$

The characteristic length of the nonlocal continuum can now be determined; however, the precise formulation of the nonlocal continuum must be specified. We consider the nonlocal continuum formulation from Bažant and Pijaudier-Cabot (1987b), in which nonlocal averaging is applied only to damage, and all other variables are treated as local. For this nonlocal damage theory, the profile of the continuum strain within the localization zone of a tensile specimen has been calculated, as shown by the graph in Fig. 8 taken from Bažant and Pijaudier-Cabot (1987b). This nonlocal formulation is equivalent in terms of energy if the area under the strain profile (curve a in Fig. 8) is the same as the area under the rectangular strain profile (curve b), which was implied in evaluating the test results according to 1. From the shape of this curve, one finds that the areas are equal if

$$h_1 = \alpha h \quad (2)$$

in which α = 1.93; and h_1 = width of the zone of localized da Furthermore, for this nonlocal continuum model (Bažant and Pijaud. ot 1987c), it has been shown that

$$h_1 = \beta l$$

in which β = 1.89. From Eqs. 1–3 it follows that

$$l = \frac{\alpha G_f}{\beta W_s} \quad (4)$$

Coefficients α and β are particular to the chosen type of nonlocal continuum formulation; for the one considered here, they yield $\alpha/\beta = 1.02$. Thus, the characteristic length is essentially the same as the width of the strain-softening zone, obtained under the assumption of a uniform strain within the zone. This is approximately true also for other variants of the nonlocal continuum formulation, and so we have, approximately

$$l \simeq \frac{G_f}{W_s} \quad (5)$$

G_f and W_s were evaluated from the results plotted Fig. 5. It was assumed that unloading followed a straight line passing through the origin, in accordance with the nonlocal model selected.

Based on the present test results, Eq. 4 yields

$$l = 2.7d_a \quad (6)$$

in which d_a = the maximum aggregate size. This is one basic result of the present study. However, verification by further tests with different aggregate sizes is desirable.

The value of the characteristic length obtained in Eq. 6 for the present experiments is consistent with previous estimates obtained when the crack-band model was proposed by Bažant and Oh (1983). At that time, the characteristic length was inferred indirectly, by using only the fracture test results and optimizing their fits for specimens of various geometries and sizes, made from different concretes. In that study, the optimum fit was obtained approximately for $l = 3d_a$.

The fracture energy, which is obtained from the unbonded test with strain localization according to the relation $G_f = U_s/A_0$, is, of course, an average value, obtained under the simplifying assumption that the fracture energy does not vary as the crack band propagates along the ligament cross section. From the value of the cross-hatched area in Fig. 5(*b*), one gets, for the present experiments, G_f = 0.0635 N/mm. This value corresponds to the work-of-fracture definition of fracture energy, as introduced for concrete by Hillerborg (1976) and used in the present RILEM recommendation (1985). From the size-effect tests, a distinctly lower value, namely G_f = 0.039 N/mm, has been previously obtained by Bažant and Pfeiffer (1987). The difference is no doubt due to the fact that the fracture energy obtained by the size-effect method has a somewhat different meaning, representing the fracture energy for the limiting case of an infinitely large specimen, in which the fracture process zone can develop without interference with the specimen boundaries and is the same for any specimen geometry.

It should be also noted that Irwin's (1958) estimate of the length of the nonlinear zone, namely

$$l_c = \frac{EG_f}{\sigma_p^2} \quad (7)$$

in which σ_p = peak stress (strength); and E = Young's elastic modulus, is sometimes also called the characteristic length (Hillerborg et al. 1976). From the presently measured values, we get

$$l_c = 8.65d_a \quad (8)$$

This value is much larger than the characteristic length l for the nonlocal continuum. The meaning of these two characteristic lengths is, of course, entirely different; l_c characterizes the length l_p of the fracture process zone ahead of the crack tip in the direction of crack propagation. (Hillerborg and Petersson have shown that $l_p \simeq l_c/2$.) On the other hand, l characterizes the effective width of the fracture process zone, governed by material heterogeneity. In the continuum description, l represents the minimum possible width of the softening zone, and in a discrete model for cracks in concrete, l represents the minimum possible spacing of discrete cracks.

It may also be noted that the minimum possible spacing of discrete cracks has been lacking from the discrete crack models used so far. This did not matter for the anlaysis of localized fracture, with a single major crack; however, for general applications, a length characterizing the minimum possible spacing of discrete cracks needs to be added to the discrete crack models of Hillerborg type (Bažant 1986).

Since the term "characteristic length" has long been established in the statistical and nonlocal theories of heterogeneous media, l_c for concrete should better be called the length (or size) of the fracture process zone or of the nonlinear zone. For metals, l_c is called the size of the yielding zone, as introduced by Irwin (1958).

Conclusions

1. The characteristic length of a nonlocal continuum that models strain-softening damage can be experimentally determined by measuring the energy dissipation in specimens in which the softening damage remains distributed and those in which it becomes localized.
2. The characteristic length of a nonlocal continuum is the ratio of the fracture energy (i.e., the energy dissipated per unit area, dimension N/m) to the energy dissipated per unit volume of the material (dimension N/m^2) (Eq. 5).
3. Distributed softening damage can be experimentally observed on concrete specimens of a rectangular cross section, whose width is approximately the minimum possible width allowed by the maximum aggregate size, and whose long sides are restrained by a layer of many thin longitudinal steel rods glued to the specimen surface.
4. The characteristic length of concrete, which may be calculated from Eqs. 4 or 5, is obtained to be about 2.7 times the maximum aggregate size.

Acknowledgments

The experiments were supported by the U.S. Air Force Office of Scientific Research under contract F49620-87-C0030DEF with Northwestern University, monitored by Dr. Spencer T. Wu, and the theoretical work was supported by the U.S. National Science Foundation under Grant MSM-8700830, monitored by Dr. Albert S. Kobayashi.

Appendix. References

Bažant, Z. P. (1976). "Instability, ductility, and size effect in strain-softening concrete." *J. Engrg. Mech. Div.*, ASCE, 102(2), 331–344; closure 104, 501–502.
Bažant, Z. P. (1982). "Crack band model for fracture of geomaterials." *Proc., 4th*

Int. Conf. on Numerical Methods in Geomechanics, Edmonton, Canada, Z. Eisenstein, ed., Vol. 3, 1137–1152.
Bažant, Z. P. (1986). "Mechanics of distributed cracking." *Appl. Mech. Rev.*, ASME, 39(5), 675–705.
Bažant, Z. P. (1987). "Stable states and paths of structures with plasticity or damage." *Structural Engineering Report No. 87-10/606s*, Dept. of Civil Engineering, Northwestern Univ., Evanston, Ill.; also (1988), *J. Engrg. Mech.*, ASCE, 114(12), 2013–2034.
Bažant, Z. P., and Oh, B. H. (1983). "Crack band theory for fracture of concrete." *Mater. Struct.*, RILEM, Paris, France, 16, 155–177.
Bažant, Z. P., and Pfeiffer, P. (1987). "Fracture energy of concrete: Its definition and determination from size effect tests." *Concrete durability, Proc. K. and B. Mather Int. Conf.*, J. Scanlon, ed., Vol. 3, 89–109.
Bažant, Z. P., and Pijaudier-Cabot, G. (1987a). "Modeling of distributed cracking by nonlocal continuum with local strain." *Proc., 4th. Int. Conf. on Numerical Methods in Fracture Mechanics*, San Antonio, Texas, A. R. Luxmoore et al., eds., Pineridge Press, Swansea, U.K., 411–432.
Bažant, Z. P., and Pijaudier-Cabot, G. (1987b). "Measurement of characteristic length of nonlocal continuum." *Report No. 87-12/498 m*, Center for Concrete and Geomaterials, Northwestern University, Evanston, Ill.
Bažant, Z. P., and Pijaudier-Cabot, G. (1987c). "Nonlocal damage: Continuum model and localization instability." *Report No. 87-2/428n-I*, Center for Concrete and Geomaterials, Northwestern University, Evanston, Ill; also *J. Appl. Mech.*, ASME, 55 (1988), 287–293.
Bažant, Z. P., and Pijaudier-Cabot, J. (1988)." Nonlocal continuum damage and measurement of characteristic length." *Mech. of Composite Materials—1988*, G. J. Dvorak and N. Laws, eds., AMD Vol. 92, ASME, 79–85 (presented at Joint ASME/SES Appl. Mech. and Eng. Sci. Conf., Berkeley, Calif., June, 1988).
Hillerborg, A., Modéer, M., and Petersson, P. E. (1976). "Analysis of crack formation and crack growth in concrete by means of fracture mechanics and finite elements." *Cement Concr. Res.*, 6(6), 773–782.
Hordijk, D. A., Reinhardt, H. W., and Cornelissen, H. A. W. (1987). "Fracture mechanics parameters of concrete from uniaxial tensile tests as influenced by specimen length." *Preprints of the SEM/RILEM Int. Conf. on Fracture of Concrete and Rock*, Houston, Tex. S. P. Shah and S. Swartz, eds., SES (Society of Experimental Mechanics), 138–149.
Irwin, G. R. (1958). "Fracture." *Encyclopaedia of physics*, Vol VI, Springer, Berlin, Germany.
L'Hermite, R. (1960). "Volume changes of concrete." *Proc., 4th Int. Symp. on the Chemistry of Cement*, Washington, D.C., 659–702.
Raiss, M. E. (1986). "Observation of the development of fracture process zone in concrete under tension," thesis presented to Imperial College, London, U.K., in partial fulfillment of the requirements for the degree of Doctor of Philosophy.
RILEM Committee 50-FMC. (1985). "Determination of the fracture energy of mortar and concrete by means of three-point-bend tests on notched beams." RILEM Draft Recommendation, *Mater. Struct.* (RILEM, Paris), 18(106), 285–290.
Rots, J. G., Hordijk, D. A., and de Borst, R. (1987). "Numerical simulation of concrete fracture in direct tension." *Proc., 4th Int. Conf. on Numerical Methods in Fracture Mechanics*, San Antonio, Tex., A. R. Luxmoore et al., eds., Pineridge Press, Swansea, U.K., 457–471.